Electronic Supplementary Information

How nanoscale surface steps promote ice growth on feldspar: microscopy observation of morphology-enhanced condensation and freezing

Raymond W. Friddle & Konrad Thürmer

Correspondence to: Raymond W. Friddle or Konrad Thürmer
Email: rwfridd@sandia.gov, kthurme@sandia.gov

Supplementary Information Text

Experimental Procedure. An icing experiment begins with adjusting the flow of the warm-fraction of the LN-cooled nitrogen stream (see Fig. S1) until the sample reaches the desired temperature (here -30°C). After settling, we found the temperature to be stable to ±1°C for about 1 hour. The vapor exiting the bubbler is bypassed to a humidity sensor prior to starting the experiment to measure the relative humidity at room temperature. This maintains a dry, cold cell chamber while the vapor stream reaches a steady state humidity. To inject water vapor, the bypass is switched to flow the vapor stream directly into the cell chamber. To stop the experiment, the vapor is again bypassed to the humidity sensor. To estimate the absolute humidity injected into the cell, AH_{in}, each run is calibrated against the saturation (RH ≈ 100 %) condition. That is, we determined the vapor flow rate, Q_{100}= 0.28 L/min, which results in the onset of condensation on the feldspar surface. We calculate the absolute humidity (g/m^3), from the measured temperature, T = -30 °C, and relative humidity, RH = 100, by the ideal gas law $n/V = P/RT$,

$$AH = \frac{P_{ws}\, M_{H20}}{R\,(T + 273.15)} \cdot \frac{RH}{100}$$

where M_{H20} = 18.02 g/mol is the molar mass of water, R = 8.314 J/K mol is the gas constant, T is in °C, and P_{ws} is the water vapor saturation pressure (in Pa) given by (Bolton 1980),

$$P_{ws} = 611.2\, e^{17.67\, T/(T+243.5)}$$

We find for the saturation condition AH_{100} = 0.45 g/m^3 at a flow rate of Q_{100} = 0.28 L/min and T = -30 °C. For constant dry cold flow rate, we assume the fraction of humid gas incorporated into the total inlet gas to be linear over the flow rates employed here (0.28 – 0.66 L/min). Therefore, for a humid line flow rate, Q, the humidity injected into the cell is approximated by,

$$AH_{in} = AH_{100}\,\frac{Q}{Q_{100}}.$$

We estimate that a 0.05 L/min error exists in our measurement of flow rate leading to an errorfor AH_{in} of ±0.08 g/m^3.

Analysis of Surface Step Segments. After background subtraction of the AFM image, a custom routine (Igor Pro, Wavemetrics) generated an interactive step-edge image (Fig. 3b of main text), where darker colors are assigned to steps larger in height. Step edges are determined from threshold-crossings (peaks) of the differentiated AFM image. The settings used detect step heights greater than 2 nm. Once a crossing is found, the peak and two floor points are used to compute the step height at that location from the original image data. The step edge location and height are assigned to a pixel on the step edge image. This process is repeated, line-by-line, along the rows and columns of the AFM image. The step-edge image is compared to the optical image of the same location showing ice formation along step edges (Fig. 3c). The interactive step-edge image allows the user to select step traces that correspond to ice-bearing step segments, shown as blue traces in (Fig. 3d). The total and selected (ice-bearing) step segments including their heights are evaluated to produce the statistical distributions shown in Fig. 4 of the main text.

Interface energy of a water wedge.

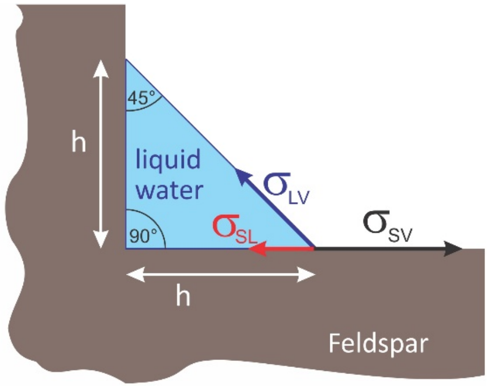

The net interface energy ΔE_{wedge} required to form a wedge-shaped water condensate of height h (see figure on the left) and length l (perpendicular to the page) is equal to the sum of all interface energies of the water wedge minus the interface energy of the feldspar surface before being covered up by the water wedge,

$$\Delta E_{wedge}/l = 2h\sigma_{SL} + \sqrt{2}h\sigma_{LV} - 2h\sigma_{SV}$$

with the specific free interface energies of the interfaces between feldspar substrate and liquid water σ_{SL}, between liquid water and vapor (humid air) σ_{LV}, and between substrate and vapor σ_{SV}.

With a contact angle of 45° Young's relation is given by

$$\sigma_{SV} = \sigma_{SL} + \cos 45°\, \sigma_{LV} = \sigma_{SL} + \frac{1}{\sqrt{2}}\sigma_{LV}$$

σ_{SV} can now be substituted in the net interface energy of the wedge yielding

$$\frac{\Delta E_{wedge}}{lh} = 2\sigma_{SL} + \sqrt{2}\sigma_{LV} - 2\left[\sigma_{SL} + \frac{1}{\sqrt{2}}\sigma_{LV}\right] = 2\sigma_{SL} + \sqrt{2}\sigma_{LV} - 2\sigma_{SL} - \sqrt{2}\sigma_{LV} = 0$$

$$\Delta E_{wedge} = 0$$

For the considered geometry, i.e., perpendicular surface steps and a contact angle of 45°, the net cost in interface energy to form a liquid water wedge of any height h vanishes. Hence, there is no nucleation barrier associated with the condensation of liquid water into such a wedge.

References

Bolton, D. (1980) *Monthly Weather Review*, 1980, **108**, 1046-1053

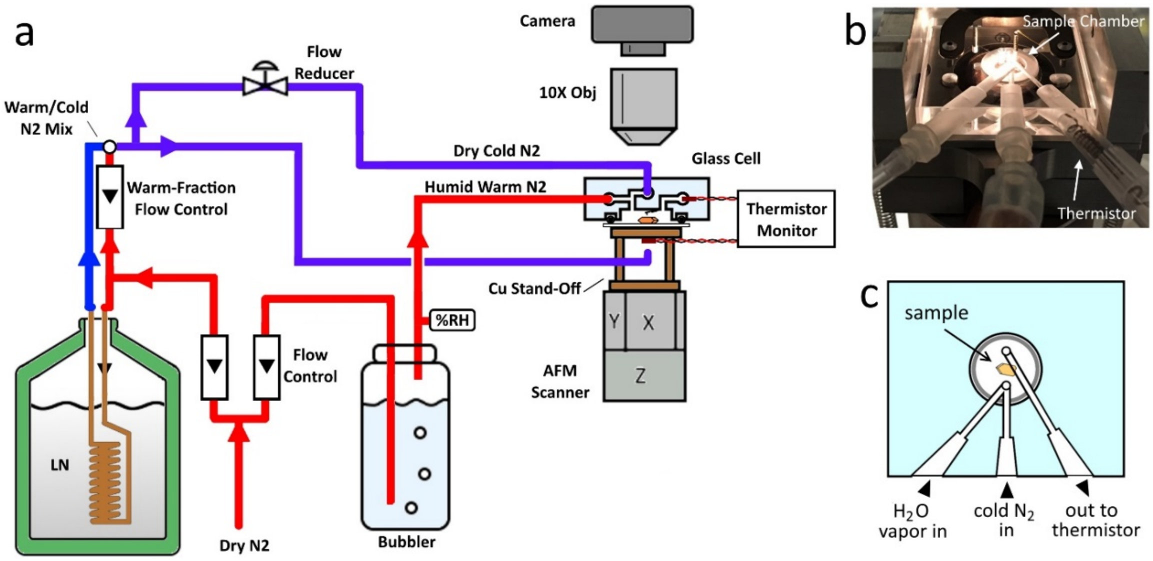

Fig. S1. Experimental setup combining environmental optical microscopy with atomic force microscopy (AFM). **a**, Flow diagram of gases: red = room temperature, blue = liquid-nitrogen cooled temperature, purple = final adjusted temperature. Dry nitrogen at room temperature flows through a heat exchanging copper coil immersed in a dewar of liquid nitrogen. The final temperature of the cooled nitrogen is controlled by mixing with room temperature nitrogen. The cooled nitrogen is then divided into two paths: one cools the underside of the copper standoff stage, and the other is piped to the inlet of the AFM sample cell. Water vapor is generated by flowing dry nitrogen through a water bubbler. The humidity of the resulting room-temperature gas is measured using a humidity sensor (ThermaData Series II – HTF, ThermoWorks). This humid nitrogen is then piped directly into the second inlet of the AFM sample cell. The AFM (Multimode 8, Bruker) is seated under a top-down optical microscopy stage with a 10X long-working-distance lens (WD = 49.5mm, NA = 0.2, resolution ≈ 1.6 μm). Video microscopy is recorded with an Infinity3-3URC 2.8 MP, 53 fps, color CCD camera. The AFM scanner, head, and objective lens are maintained in a dry nitrogen environment by an acrylic atmospheric hood (MMAH2, Bruker, not shown). A copper standoff stage creates space between the sample and the AFM scanner for underside cooling and thermistor placement. Temperature is monitored by thermistors placed at the underside of the copper standoff and the outlet of the sample cell (see panels b and c). The thermistor readings are recorded in real time with a TC-720 thermoelectric temperature controller (TE Technology, Inc.). **b,c**, The atmospheric-pressure environmental chamber consists of a glass electrochemical AFM liquid cell (model ECFC, Bruker). Cold dry nitrogen and room temperature humid nitrogen are mixed inside the chamber to create the atmospheric conditions for ice formation. The two gas-inlet ports meet at the entrance to the sample volume. This allows separation of cold N2 and water vapor until the moment they enter the cell, preventing ice formation and clogging of the supply lines.

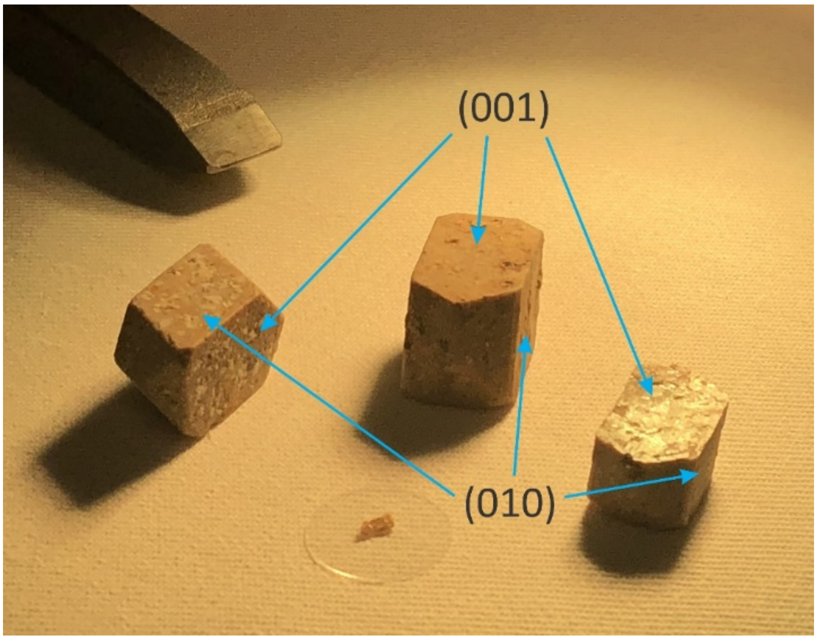

Fig. S2. Sample preparation. The substrates were prepared by mechanically splitting crystals of K-feldspar (Orthoclase, $KAlSi_3O_8$, source: Yavapai County, Arizona, USA, vendor: VWR/Eric Miller) along the easy-cleavage (001) plane. After cleaving single feldspar crystals with a Tungsten carbide-tipped steel chisel, the resulting small fragments are glued to a glass slide with thermally conductive epoxy. The same thermally conductive epoxy is used to adhere the glass slide to the copper stand-off stage.

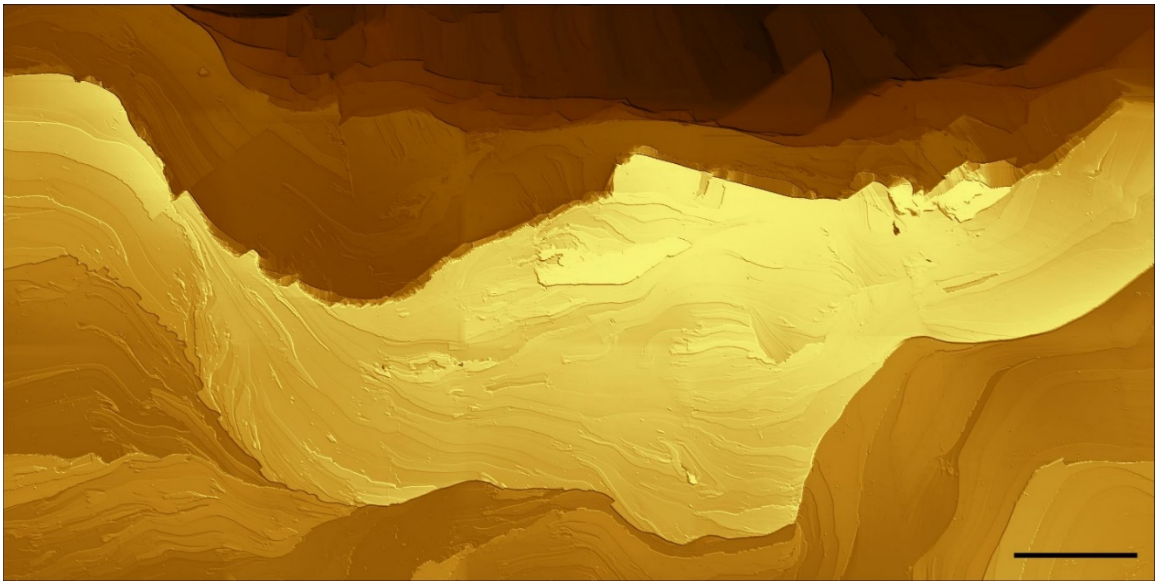

Fig. S3. Detailed topographic map of the examined K-feldspar surface. This map is produced by stitching together 15 individual AFM images, each with a 100x100 μm^2 field of view (FOV). Typically, image borders overlapped 10 μm with neighboring images. Borders are seamed by alpha blending such that the image height, h_i, across the overlap of images i = 1,2 is given by $h_{tot} = \alpha\, h_1 + (1 - \alpha)\, h_2$., where α varies from 0 to 1 across the width of the overlap. The area displayed is 466 x 233 μm^2, and corresponds to the region of the video microscopy data used in analyzing iced step-height statistics. Note that the actual analysis of step heights is performed on the original individual images to avoid errors caused by seams. To improve visibility of small steps, a "false light" shading (Gwyddion) is applied here. Image stitching is performed using a custom routine (Igor Pro, Wavemetrics). Scale bar 50 μm.

Fig. S4. Ice bands on the (010) face of feldspar. The image shows an optical frame from an experiment performed on the (010) face at -25°C under AH_{in} = 1.18 g/m^3. As in the case of the (001) face, dark bands extending across the image are ice, which abruptly appeared and immediately started consuming the small droplets of liquid water that had initially covered the entire surface.

Supplementary Movies

Movie S1. Optical video of ice growth on feldspar at T= -30°C and AH_{in} = 0.45 g/m^3, corresponding to frames in Fig. 1A of the main text. Field of view is approximately 404 μm x 250 μm.

Movie S2. Optical video of ice growth on feldspar at T= -30°C and AH_{in} = 0.75 g/m^3, corresponding to frames in Fig. 1D of the main text. Field of view is approximately 404 μm x 250 μm.

Movie S3. Optical video is thresholded and shown as a false-color overlay on an AFM mosaic. Video data is taken at T= -30°C and AH_{in} = 0.75 g/m^3. Field of view is approximately 220 μm x 425 μm.

Movie S4. Optical video of ice growth on feldspar at T= -30°C and AH_{in} = 0.75 g/m^3, corresponding to frame in Fig. 2C of the main text. Field of view is approximately 230 μm x 310 μm.

Movie S5. Optical video of ice growth on feldspar at T= -30°C and AH_{in} = 0.90 g/m^3, corresponding to frame in Fig. 2D of the main text. Field of view is approximately 230 μm x 310 μm.

Movie S6. Optical video of ice growth on feldspar at T= -30°C and AH_{in} = 1.05 g/m^3, corresponding to frame in Fig. 2E of the main text. Field of view is approximately 230 μm x 310 μm.